PROCEEDINGS, 50th Workshop on Geothermal Reservoir Engineering
Stanford University, Stanford, California, February 10-12, 2025
SGP-TR-229

Lessons from Utah FORGE for Seismic Monitoring of Engineered Geothermal Systems

Kristine Pankow, Ben Dyer, James Rutledge, Dimitrios Karvounis, Peter Niemz, Katherine Whidden, Peter Meier, Paul Jaques, Gesa Petersen, David Eaton, Julie Shemeta, and Joe Moore

University of Utah Seismograph Stations, Salt Lake City, Utah; Geo Energie Suisse, Zurich, Switzerland; Santa Fe Seismic, LLC, Sante Fe, New Mexico; GFZ, Potsdam, Germany; MEQ Geo Inc., Denver, CO; University of Calgary, Calgary, Alberta, and EGI, University of Utah, Salt Lake City, UT

kris.pankow@utah.edu; b.dyer@geo-energie.ch; rutledge@swcp.com; d.karvounis@geo-energie.ch; peter.niemz@utah.edu; katherine.whidden@utah.edu; p.meirer@geo-energie.ch; paul@geoware.co.uk; gesap@gfz.de; eatond@ucalgary.ca; julie@meqgeo.com; and jmoore@egi.utah.edu

Keywords: Seismic Monitoring, Utah FORGE

ABSTRACT

There are two goals for seismic monitoring of Enhanced Geothermal Systems (EGS): (1) monitoring for seismic risk (triggering traffic light systems) and (2) characterizing reservoir development. For seismic risk, the emphasis is on accurate magnitude and ground-motion observations. For reservoir development, the emphasis is on microseismic event detection and high precision location. At the Utah Frontier Observatory for Research in Geothermal Energy (FORGE), we are testing seismic instrumentation, seismic array configurations, and enhanced seismic processing algorithms. With each operational phase, we prepare a seismic monitoring plan and at the completion of each phase, we evaluate the effectiveness of the seismic monitoring and identify lessons learned to be implemented in the next operational phase. Here, we summarize the evolution of seismic monitoring at Utah FORGE and identify lessons learned. Based on this experience, we make some general recommendations for future seismic monitoring at Utah FORGE that may also be considered for other EGS projects.

1. INTRODUCTION

The mission of the Utah Frontier Observatory for Research in Geothermal Energy (FORGE) project is to develop the technologies that are necessary for de-risking Enhanced Geothermal Systems (EGS). Seismic monitoring and research into enhanced seismic monitoring promotes this mission through safety protocols managed with Traffic Light Systems (TLS) and by imaging reservoir development. These end member uses of seismic monitoring rely on different aspects of the seismic wavefield. For traditional TLS monitoring, the key parameters are magnitude and ground motion. For monitoring the reservoir, the key parameters are related to microseismic event detection and high precision location. Between these end member cases seismic monitoring is used for adaptive TLS and three- and four-dimensional seismic velocity inversions. At Utah FORGE, we designed multi-scaled seismic networks in order to obtain the data necessary for seismic monitoring and research across the end member needs.

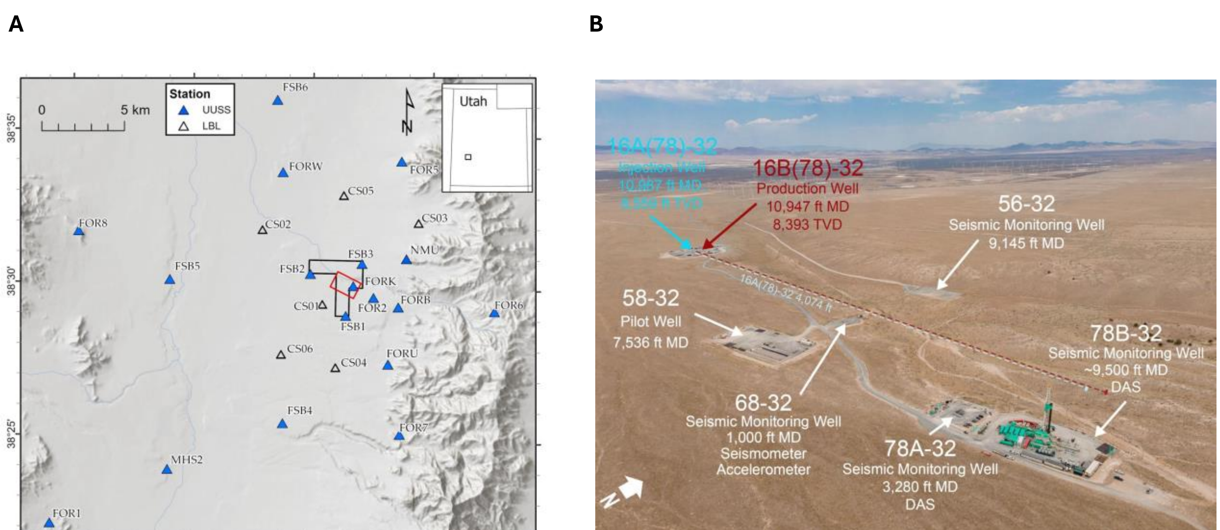

Figure 1: (A) Map of the Utah FORGE local seismic network. Blue triangles: stations operated and maintained by Utah FORGE. Station FORK is a 300 m borehole; stations beginning with FSB are in 30 to 40 m deep postholes; and stations beginning with FOR are located on the surface. Open triangles are stations operated by Lawrence Berkeley National Lab (Chet Hopps, 2023). These stations are not used in Utah FORGE routine processing but are shown for reference. The black polygon is the original outline of Utah FORGE; the red polygon, the approximate location of area shown in (B). (B) Aerial photograph showing the locations of the deep boreholes used for seismic monitoring. Well 68-32 is the location of station FORK.

The backbone of the seismic network at Utah FORGE is a local scale seismic network composed of seismometers and accelerometers located at the surface and in shallow postholes (30 - 40 m) (Figure 1A). There is also one station, FORK, located in a shallow borehole (300 m). This station is exceptionally valuable in detecting seismic activity within the reservoir. This local network is embedded into the Utah Regional Seismic Network (Pankow et al., 2019) and data is telemetered in near-real time to the University of Utah. This data flows into an Advanced National Seismic System EarthQuake Monitoring System (AQMS) where events are built, located, and alarms are issued based on the Utah FORGE TLS (Pankow et al., 2024). Appendix 1 details the evolution of this network and describes the metadata. All data from this network are archived at the EarthScope Data Management Center (DMC).

In addition to the local network, Utah FORGE designed and drilled a network of reservoir depth boreholes to be used for seismic monitoring and high temperature tool testing (Figure 1B). The geometry of the wells was informed by modeling for microseismic detection and location (Dyer et al., 2010; Freudenreich et al., 2012). These wells may be instrumented during Utah FORGE operational activities (Table 1). The resolution capability of the downhole networks is illustrated in Figure 2 showing the distinct event lineaments that may be interpreted from the April 2024 16A(78)-32 stimulation. Before each operation, the goals for seismic monitoring are defined and various configurations for sensor placement modeled. Appendix 2 describes the borehole seismic network for operational phases listed in Table 1. Seismic data from the operational phases has been submitted to the Geothermal Data Repository for archiving.

Table 1: Utah FORGE operational activities.

Date	Operational Goals
2019 April	58-32 Stimulation--can we create fractures? Can we detect stimulation microseismicity near and above the granite/basin-fill interface?
2021 January	Injection well 16A(78)-32 drilled
2022 April	16A(78)-32 Stimulation—where to drill the production well?
2023 June	Production well 16A(78)-32 drilled
2023 July	Circulation test—are the injection and production wells connected?
2024 April	16A(78)-32 and 16B(78)-32 Stimulation—can we develop a commercial scale reservoir?
2024 August	Month long circulation—how much fluid can we recover?

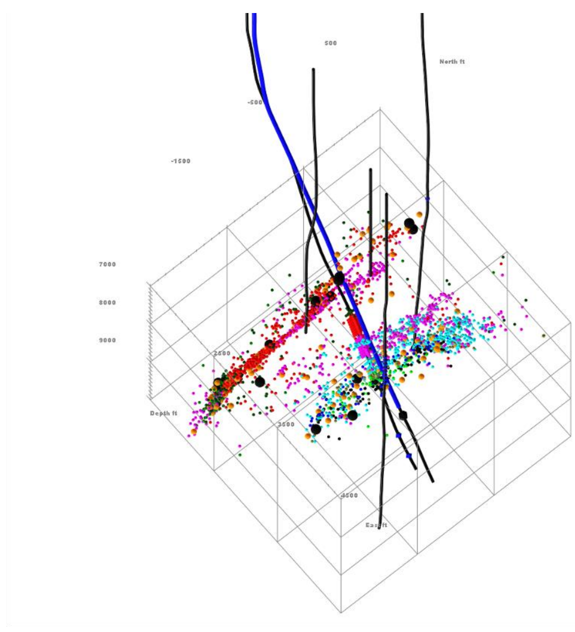

Figure 2: 3D view of the April 2024 16A(78)-32 stimulation events that have been reviewed. The symbols are colour coded according to the stimulation stage in 16A(78)-32. Orange symbols are events >0.6Mw and black symbols are events >1.0Mw. The maximum event was 1.9 Mw. The injection and production wells are shown as inclined black and blue wells, respectively. Vertical black lines show the locations of the other deep monitoring boreholes relative to the seismicity.

A third component of the seismic network utilized at Utah FORGE are large-nodal geophone deployments (Figure 3). The Fairfield nodal geophones used by Utah FORGE are deployed in month-long intervals (the duration of the battery). Each deployment is for a specific experiment. Experiments have been conducted to determine the seismic velocity structure, for improving the microseismic event detection and location, and to facilitate studies of microseismic source properties. Appendix 3 describes the nodal experiments conducted by Utah FORGE. Data from these experiments are archived at the EarthScope DMC.

From these varied seismic monitoring initiatives, Utah FORGE learned many lessons. Here we discuss the lessons learned and how these lessons are incorporated into new phases of seismic monitoring at Utah FORGE.

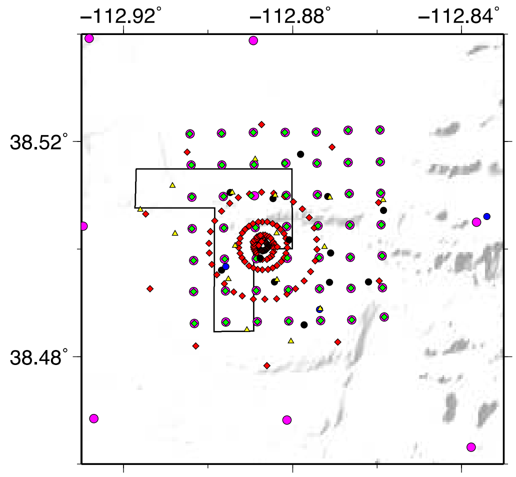

Figure 3. Array geometries from past nodal experiments. Symbols denote three separate deployments: pink circles: a rectangular array (49 geophones with 650 m spacing) deployed in 2016; red diamonds: 5 concentric ring arrays (151 geophones, with radii of 100 m (first ring) and 2500 m (second ring)) deployed to monitor the 2019 stimulation; black circles: location of geophone patches deployed in 2022 (each patch had a rectangular grid of 16 geophones (internal patch spacing 30 m)); yellow triangles: location of geophone patches deployed in 2024 (each patch had a rectangular grid of 9 geophones (internal patch spacing 10 m)).

2. SEISMIC INSTRUMENTATION IN EXTREME ENVIRONMENTS

2.1 Borehole Instruments

To maximize the sensitivity and resolution of the borehole network, the sensors needed to be installed in monitoring wells at reservoir depth based on modelling of the network resolution. The principal consideration in selecting the seismic tools was their temperature rating due to the high temperatures at relatively shallow depths at Utah FORGE compared to normal oilfield applications of borehole seismic tools. Consequently, the potential deployment depths of the tools were constrained by their temperature ratings rather than their pressure ratings. A further factor in specifying the seismic monitoring equipment was the connection of the downhole tools to the surface. In the case of the geophone tools, a 7-conductor wireline was used. For fiber optic tools, either a fiber optic wireline or behind casing fiber in metal tubing (FIMT) was required. The performance of these two distinct types of systems, electronic geophones/accelerometers and fiber optic, was assessed during various stimulation and circulation tests between April 2022 and September 2024, as discussed below.

2.2 Geophones and Accelerometers

Three systems were tested: multi-level, digital geophone and accelerometer strings and a two-level analogue geophone tool. The first monitoring phases in April 2022 were conducted using eight-level, 3 component (3C) digital geophone strings with the two-level 3C geophone strings as backup. These tools had temperature ratings of 195°C and 225°C respectively and were deployed on wireline rated at 260°C. The plan was to deploy an eight-level string in each of the three monitoring wells.

The string and a backup string that were deployed in well 56-32 encountered multiple problems such that it was not possible to establish a single cause of the failures. However, the tools that were deployed in the other two monitoring wells, 58-32 and 78B-32, performed better and enabled some operational parameters to be established. Principally, what was found was that the cooling capacity of the tools was not as efficient as expected and it was not possible to run the tools at greater than 180°C ambient borehole temperature. This corresponded to an internal tool temperature of 160°C above which, at greater tool depths, the electronics of the tools shut down. It was also found during these first deployments that there was gas present in well 56-32, which was also witnessed later in the other two monitoring wells. This may have been a factor reducing the reliability of the cablehead terminations. Multi-level tools were particularly susceptible to cablehead problems due to the number of cableheads that are required to make up the string with an interlinking cable between each 3C geophone section and the next. Due to the difficulties of deploying a geophone string in well 56-32 during the April 2022 stimulation, a two-level analogue system (PSS tools) was deployed at 7315ft and 8315ft below ground level (bGL) corresponding to temperatures of 193°C and 212°C respectively. These tools only lasted 3 days but at least demonstrated their potential for high temperature deployment. However, as they were intended for long term monitoring significant improvements in reliability were required.

Following the April 2022 stimulation various attempts were made to deploy the analogue tools. Unfortunately, all ended in immediate failure. In an effort to establish the causes of the failures, stepwise testing of the analogue PSS tools was conducted in October 2023. This work commenced with rigorous preparation of the tools overseen by a consultant logging engineer. One of the potential problems that had been identified from earlier experience was the presence of water droplets within several of the tool bodies. This could be due to condensation as the tools were assembled in the rather damp atmosphere of southwest England or to the use of spring energized seals in place of one of the two elastomer O rings of the cableheads. Hence, a procedure was specified for the tool preparation that included baking the tools, flushing with inert gas, and fitting the cableheads so that the electronics were dry and sealed prior to sending to site. During the preparation, the cleanliness and surface of the O ring seats were also strictly checked. The spring energized seals were replaced with O rings and the O rings were updated to an elastomer type with greater resistance to gas and that retained greater flexibility at temperature.

Cablehead electrical breakdowns affected both the digital geophone strings and the analogue tools. These were traced to misfitting of the elastomer insulators (referred to as boots) over the pins (referred to as feed throughs) that are used to terminate the conductors in the wireline at each cablehead. The potential for this occurring was practically eliminated with a new design of fitting tool to push the boots over the feed throughs. A further factor in premature breakdown of the cablehead insulation may have been due to the wireline. It was noted that one of the wirelines used contained a conductive tape around the electrical conductors. This tape is present for convenience in the construction of the wireline and is not stable at Utah FORGE downhole temperatures. At these high temperatures, the tape broke down into a conductive powder within the cableheads. It was not established if this was significant but was easily avoided by specifying a different wireline construction without the tape.

Following the changes in practice defined above it was found that the analogue tools were far more reliable. Most recently, an analogue tool was deployed for nine months before performance decayed. However, this improvement in reliability revealed a faulty electronic component that caused electrical spikes that were unlikely to have been detected previously but has been corrected now. There are a couple of other points that should be borne in mind with respect to these tools. Firstly, the elastomer seals do not work properly in the cold so the tools should be kept indoors until needed. Secondly, at the Utah FORGE site the surface installations for the tools must be protected to prevent rodents chewing on the wires and damaging them.

2.3 Fiber Optic Tools

Since in principle fiber optics can operate at considerably higher temperatures than geophones, three fiber optic sensor configurations have been tested for seismic monitoring. First is a three component (3C), three level clamped sensor string. Second is a fiber cemented behind casing, and third is a wireline DAS. The most sensitive of these systems was the 3C string. However, this string requires significant development to improve vector fidelity and of the interrogator/data acquisition system at the surface. This development is underway.

Single and multimode fibers for monitoring strain (Distributed Strain Sensing (DSS)), seismicity (Distributed Acoustic Sensing (DAS)) and temperature (Distributed Temperature Sensing (DTS)) were deployed in fiber optic cables in two of the seismic monitoring wells: in well 78-32 to the bottom of the well (TD), a depth of 3273 ft and in 78B-32 to a depth of 3915ft with ~1,300 ft in the granite. An attempt to install DAS behind casing in the monitoring well 56-32 was unsuccessful. The DAS fiber is contained in a metal tube referred to as Fiber in Metal Tube (FIMT). The experience in well 56-32 and to a lesser extent 78B-32 whereby the FIMT was broken above TD illustrated the risk of damaging the FIMT during the installation of the casing.

Three different fiber optic cables were deployed in the annulus of the 7” casing in 16B(78)-32. Two separate cables for monitoring DAS, DSS, and DTS were run by the University of Texas at Austin and Rice University. A third cable attached to a pressure-temperature gauge were located at the heel of the well. During the installation metal shields were placed over the cables to protect them and logs were run to determine their locations prior to stimulating the well. The installation was overseen by an expert with extensive experience in the deployment of fiber optic cables. This was clearly a critical contribution.

Good data was acquired from the 16B(78)-32 DAS during a number of stimulation and circulation tests at Utah FORGE and at the nearby Fervo Cape Modern site. A comparison of the response of the 16B(78)-32 DAS with 3C geophone data is shown in Figure 4. Although the signal to noise ratio of the DAS is only around a tenth of that of the 3C geophones, the continuity of the DAS data from trace to trace and the wide aperture of the array make the DAS data very well suited to autolocation. During the stimulations in 16B(78)-32, the maximum depth of the active portion of the FIMT was progressively reduced as the stimulation zones moved up the borehole. During this period the FIMT was breached, and fluid was pushed up the FIMT emerging at the surface connection. The unfortunate downside of deploying a FIMT behind casing is that it is not repairable and cannot be replaced.

In principle, DAS can also be acquired using a FIMT contained within a wireline that is temporarily installed within a well. Coupling to the casing may be achieved if the well has a small inclination, but to ensure coupling another approach is to run some slack wireline into the well so that the wireline spirals up the inside of the casing. In April 2024, a wireline DAS was deployed in well 58-32. This well was flowing small quantities of gas-rich fluid and would pressurize when shut-in. Hence the wireline was deployed through a pack-off so that the well could be closed with the wireline downhole. To be able to run slack into the well, the wireline must be terminated with a clamped tool. As there were no electrical connections in the wireline, the clamping arm was held in the closed position by a dissolvable pin that released the arm after 24hrs and clamped the tool to the casing. Once the tool was locked to the casing, a few 10s of ft of wireline could be run into the well such that the wireline contacted the casing. By observation, this approach seems to have worked and comparable signal to noise was obtained on the wireline DAS as from the behind casing DAS in 16B(78)-32 (Figure 5).

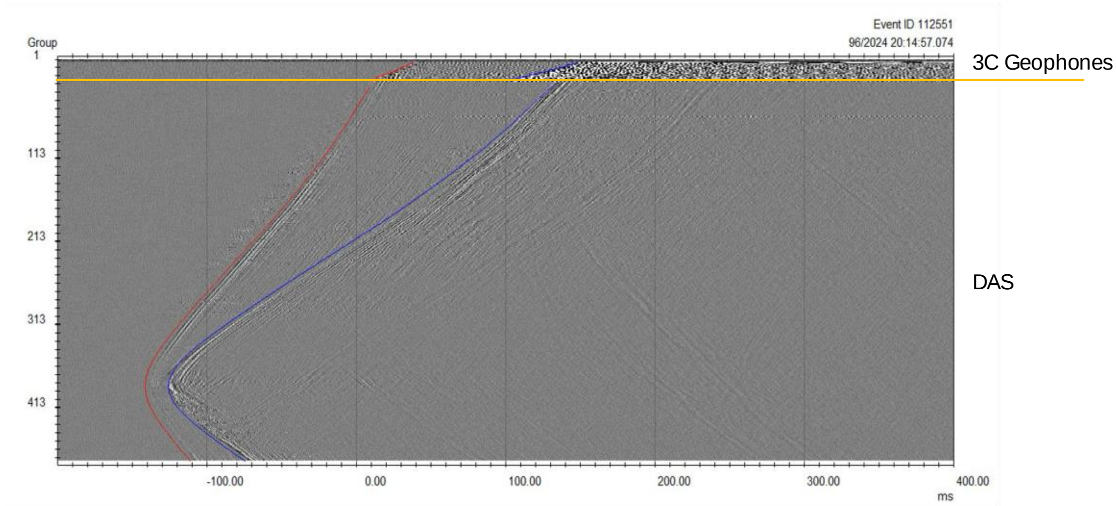

Figure 4. Illustration of the relative signal of the DAS data (Groups 10 – 520) compared to the 3C geophones (Groups 1 - 9). Although the sensitivity of the DAS is significantly less than the geophones the continuity across the DAS array enable the P (redline) and S (blue line) to be reliably interpreted.

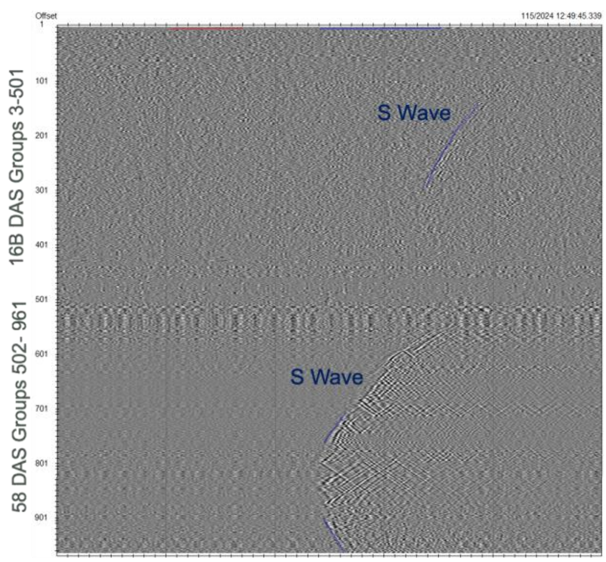

Figure 5. Comparison of the response of the wireline DAS deployed in well 58-32 vs the behind casing DAS in 16B(78)-32. The wireline DAS was deployed after the 16B(78)-32 stage 4 stimulation and only detected a few events prior to the circulation test. This event was selected as it is of similar offset from 58-32 as it is from 16B(78)-32.

Regardless of whether the well is inclined or not, the FIMT still needs to be terminated in a pressure housing to prevent fluid from entering the FIMT. The clamped tool at the end of the wireline served this purpose. A feature of this tool was that it only used metal to metal type seals. This was an important development towards long term reliability of downhole tools in comparison to conventional elastomer type seals that may break down at the higher temperatures of geothermal applications.

Additionally, in acquiring DAS data, special care must be taken regarding the Interrogator Unit (IU). IUs are temperature sensitive. Careful control of room conditions is needed. It is important to keep the IUs in an insulated room with Air Conditioning. It is also important to maintain the A/C unit.

3. REAL TIME SEISMIC MONITORING

3.1 Borehole Network

During the April 2024 stimulations, the borehole network consisted of the PSS in 56-32 (3 channels), the Geochain in 78B-32 (24 channels), the DAS behind casing system in 16B(78)-32 (1496 channels), and a behind casing DAS system in monitoring well “Delano” (1317 channels) on the Cape Modern project area being developed by Fervo. The sampling rate of the three component (3C) PSS and Geochain sensors was set at 4 kHz and the two DAS systems, 16B(78)-32 and Delano were run at 10kHz. Data from the DAS system was collected at a rate of approximately 0.8 Gbps. More than 8 TB of raw DAS data were generated per day. Management related to the large

DAS data volumes was a challenge. Designing a borehole monitoring network with multiple DAS requires planning in advance for the necessary hardware and the characteristics of the communications network. One needs to estimate the amount of data expected to transfer through the network, the minimum read and write speed of the hard drives, and how the storage space of these hard drives balances with the reliability of their underlying technology (e.g. Solid State Drives (SSD) or Hard Disk Drives (HDD) technology or cloud services).

Some downtime in processing seismic data is unavoidable, and when recording DAS during these downtimes the volume of unprocessed DAS data collects quickly. To reduce downtime, it was found to be important to maintain the necessary personnel on site (i.e. IT experts and software developers). Fast solutions related to downtime need to be developed and implemented before the data volume causes further issues (e.g. shortage of storage). Solutions may include relocating IU to wellpads with different data storage capacities and network characteristics or implementing new IU that export data differently (e.g. different file or directory structures).

While raw DAS files need to be securely stored and easily accessible if reprocessing is needed, simply mirroring the destination path, where raw DAS files are copied is suboptimal and can lead to data latency issues. The time needed for mirroring increases as the number of files in the source path increases and does not allow removing files from the destination. Forwarding operations that sequentially copy all the seismic files stored in the source path is preferable. Files that have been successfully copied to the destination path are not revisited again or compared with the file in the source path. When forwarding, resuming copying from the last copied file is possible and files can be copied with a controlled frequency. Robust workflows for file handling and storage are important and should be designed in advance of processing with technical experts.

Making archives of the important seismic data also needs time and the correct storage solutions. Solid State Drives (SSD) read and write faster than typical Hard Disk Drives (HDD) and are recommended for files with data that need to be processed in real time. HDDs and solutions with Redundant Array of Independent Disks (RAID) are a reliable solution for longer term storage of seismic files as hardware failures are less likely. An inventory of SSD and HDD hard drives and the type of archive data is needed in advance of operations. HDDs are mobile, readily available and do not require a reliable Internet connection. However, a disadvantage is that external HDDs can be filled with uncompressed continuous DAS data in days. Also, copying DAS data files can take a considerable amount of time that depends not only on the total size of data in the HDD but also on the number of files.

In processing DAS data, reading and writing of a large file with DAS data is not easy to parallelize and instead optimized serial algorithms are needed. Processing tasks can benefit from scalable algorithms and can be increasingly fast as the number of CPU cores increases or when GPU parallelization is employed. But this is not the case for the read and write operations. It was found that first copying large files with DAS data to a local SSD from a Network Attached Storage (NAS) is faster than reading the same file directly from the NAS. This seems to be mainly because the process of copying data without reading is very efficiently programmed in the operating systems.

Parallelizing a code is important for the algorithms processing the DAS signal. DAS can be deployed at depths near the stimulation where microseismicity occurs. The range of frequencies needed to be resolved scales with the distance to the microseismic events. DAS systems can sample up to 10 kHz in real time and resolve these wavelengths with many samples for many hundreds of different channels. Pre-processing these channels in parallel is a necessary efficiency needed for real time monitoring. There are many available libraries that are parallelized. However, since the actual coding is not always apparent, these tools also come with the increased risk of overhead. During operations, the more overhead that exists with external software, the more time it takes to resume operations, and the less flexible the workflow can be to network changes. One needs to be aware of the thread safety of these libraries, how much time it will take to install in a new computer, how to best use it when different user input is required or when it needs to be updated with a newer version.

Finally, DAS can operate with a minimal latency and supplement a TLS alert if necessary. DAS fibers seem to be less sensitive than the 3C downhole sensors but are sensitive enough for detecting and locating events important for a TLS decision. However, a weakness and potential research and development opportunity of DAS is the inability to calculate magnitude. Using magnitudes from other seismic monitoring, DAS systems can be used to quickly approximate the depth and the source time of events with strong signal and with high confidence even when seismicity occurs with high frequency.

3.2 Surface and Near-Surface Monitoring

The local permanent seismic network at Utah FORGE expanded and improved over time (Figure A1.1). In its current state, it consists of 10 surface stations and 6 shallow borehole instruments at depths of ~30 m to ~305 m (Appendix 1), covering distances between 0 and 20 km around Utah FORGE. Data from the local network is embedded into the Utah Regional Seismic Network (Pankow et al., 2019) and data flows in near-real time into an AQMS operating system where events are built, located, and alarms are issued above pre-defined magnitude thresholds. This network and processing schema are designed to monitor seismic risk (TLS) and the emphasis is on constraining magnitude and ground motion. Within AQMS, events are located using a one-dimensional velocity model. Because of the westward dipping granite-basin fill interface, epicentral locations bias to the east. The magnitudes are consistent with the Utah Regional Seismic Network calibrated magnitudes (Pechmann et al., 2007) providing a uniform magnitude scale for comparison.

This original design for network operations at the University of Utah Seismograph Stations has been overwhelmed by activities supporting Fervo's Cape Modern project. To ensure both regional and local seismic monitoring, operations are being modified. Utah FORGE data will flow into a separate AQMS instance with a subset of the data flowing into the regional AQMS instance. The regional instance will produce a catalog with a magnitude of completeness (M*c)* of at least 1.5. This is sufficient for driving the alarms necessary for the Utah FORGE TLS. The Utah FORGE AQMS instance will create an automatic catalog to much lower magnitude that can be accessed for research purposes. We have also integrated a second enhanced data processing schema into operations that is described in the next section.

4. ADVANCED DATA PROCESSING

On the one hand, the detection capability and the resolution of (near-)surface networks are more limited compared to downhole monitoring networks due to the larger distance to the geothermal reservoir and a noisier sensor environment. On the other hand, the (near-)surface seismic network provides continuous recordings spanning multiple years in contrast to the campaign-style deployment/usage of downhole monitoring at Utah FORGE. To overcome the reduced resolution of the surface seismic network, a joint workflow of full-waveform-based enhanced detections and relative relocations was implemented.

Data collected by the local network between April and August 2023 were used as a test case and benchmark for the newly developed detection and locations algorithm *qseek* (Isken et al., 2025). *qseek* improves the full-waveform-based detection workflow by combining machine-learning-informed phase detection with robust migration and stacking techniques. With the support of 3D velocity models, *qseek* maximizes the information gained from surface monitoring. In our case, the enhanced automatic earthquake detection workflow relies on a subset of only five permanent seismic stations closest to the injections and a local 3D velocity model (Finger et al., 2024). The enhanced detection workflow lowers the detection threshold compared to the regional catalog produced by UUSS by about one magnitude. It can detect events as small as M -2 in quiet periods and M -1 in wind-induced high-noise periods (Niemz et al., 2024, Niemz et al., 2025). The enhanced workflow for waveform-based event detection revealed minor seismic activity induced during drilling and increased induced seismic activity during the 2023 circulation test (Figure 6). There was no complementary downhole geophone monitoring during this circulation and the (near-)surface monitoring is the only comprehensive dataset that could provide reliable microseismic event locations for the entire period of the circulation tests (Niemz et al., 2024). The detection-and-location workflow runs in quasi-real time and provides reliable detections and preliminary locations.

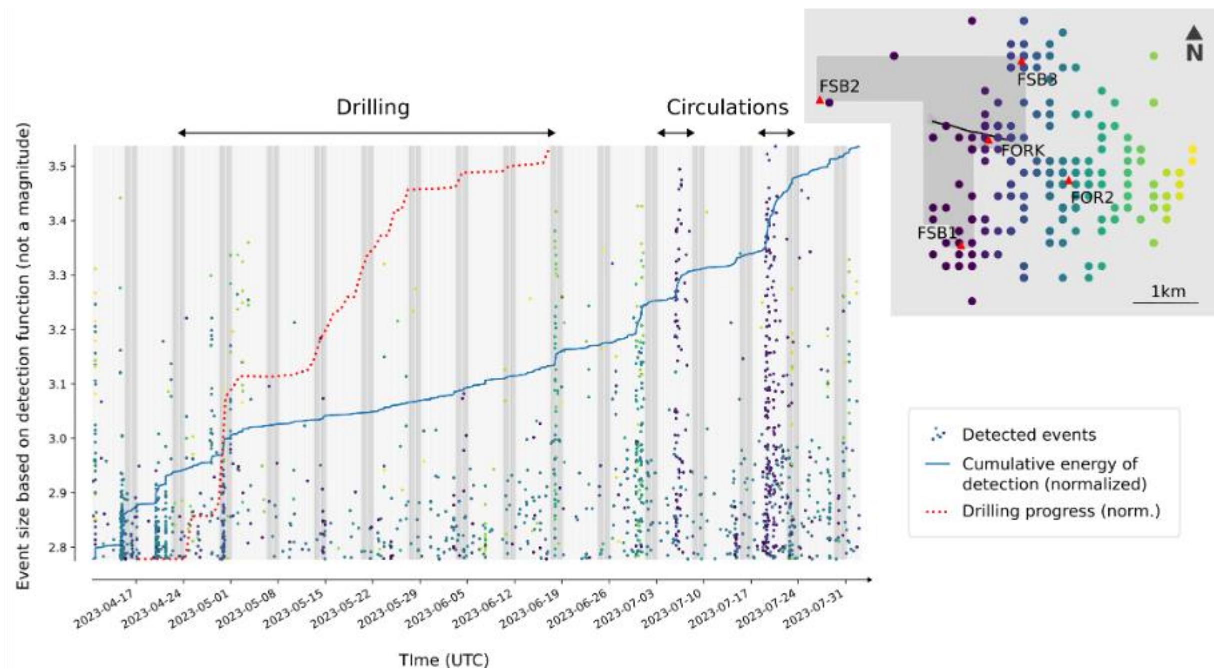

Figure 6: Enhanced earthquake detection between April and August 2023. The detected events are colored by longitude to separate events below the Utah FORGE site (purple) and natural seismicity (green to yellow) to the east, close to Blundell geothermal power plant or in the Mineral Mountains. For convenience, gray bars in the background of the timeline divide the data into weeks, without any implications for the seismic activity.

To further improve the location quality, we relocated subsets of the surface-based microseismic event detections using the relative relocation algorithm GrowClust (Trugman and Shearer, 2017; Trugman et al., 2022), including the 2022 stimulation, the 2023 circulation, and the 2024 stimulation. Subsequently, we match the results for the 2022 stimulation with the high-quality locations of the 2022 downhole catalog of Dyer et al. (2023), to obtain absolute locations. The locations of over 500 events induced during the in 2023 circulation map the further growth of the fracture zone opened during stage 3 of the 2022 stimulation (Niemz et al., 2024). The relocation of events during the 2024 stimulation, incorporating temporary nodal geophone data (see next section) for the 2024 stimulation, showed a repeated reactivation of the fracture zone from 2022 and a newly induced fracture zone (Niemz et al., 2025).

5. NODAL GEOPHONE EXPERIMENTS

Temporary geophone experiments provide useful supplemental data to the permanent seismic network. These experiments can provide for a more dense and uniform station coverage. These data are especially useful in velocity model studies and can provide the dense coverage needed for seismic source studies and improved location. At Utah FORGE, we have experimented with different deployment geometries (Figure 3) and methods of installation. The first experiments (Appendix 3) with rectangular geometries proved useful for determining the local (Trow et al. 2018; Zhang et al., 2021) and regional (Wells et al., 2022) velocity structure. However, this rectangular geometry and the circular arrays provided only marginal improvements for location and source studies of induced seismicity. The wind at Utah FORGE is a constant noise source and the effect on single nodes is evident.

To mitigate the effect of the wind and other local noise sources, we installed the nodes in patches in 2022. The goal was to stack the data across each patch (Whidden et al., 2023) for SNR improvements. For this experiment, we used 16 nodes separated by 30 m in a 4 x 4 grid. The sensors were partially buried so that the top of the instruments were flush with the ground surface. From the 2022 stimulation, we learned that the spacing was not optimal for stacking seismic phases for the dominant frequencies of the recorded events. Additionally, several individual nodes had high noise levels.

In May 2023, we deployed 76 nodal instruments with the goal of optimizing nodal spacing within each patch and burial depth (Niemz et al., 2023). The deployment consisted of two nodal patches relocated at patch locations from the 2022 deployment (Figure 7). In this experiment the nodes were spaced 5-10 m apart. We stacked event data using spacings of 5, 10, and 20 m (Figure 8). The optimal spacing was determined to be 10 m. We also varied the nodal burial depth from flush with the surface (same as 2022), 5 cm deep, or 10 cm deep. Results show a decrease in background noise level of the nodes, especially a decrease in correlated wind noise for the fully buried nodes (Figure 8). Using the lessons learned from this experiment, for the 2024 experiment, all nodes were fully buried and we opted for 16 patches of 9 nodes separated by 10 m in a 3 x 3 grid. Niemz et al. (2025) show that this patch configuration produces signal equal to or in some cases better than broadband sensors deployed in shallow (30 m) postholes. Decreasing the number of nodes per patch from 16 to 9 also allowed us to increase the number of patches that could be deployed with the available nodes improving focal sphere coverage.

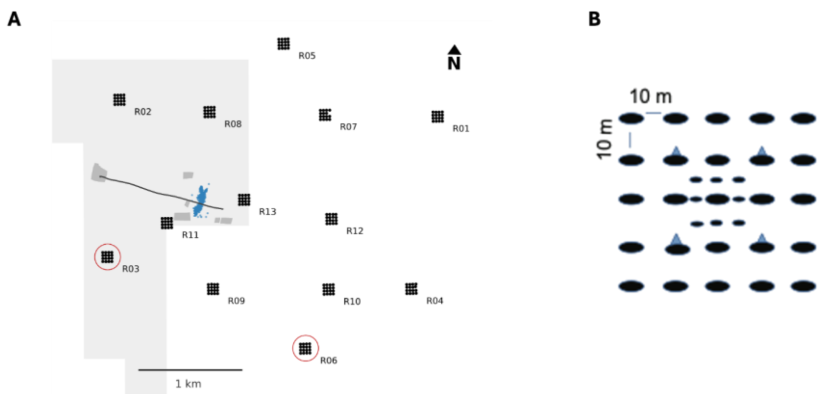

Figure 7. A. Geometry of the 2022 nodal deployment at the Utah FORGE site, with 2023 patch locations indicated by red circles at patches R03 and R06. The surface projection of well 16A(78)-32 is shown as a solid line. The microseismic activity from 2022 (Dyer et al., 2023a) is shown in blue. B. Detail of the 2023 patch geometry with 5-10 m spacing between nodes.

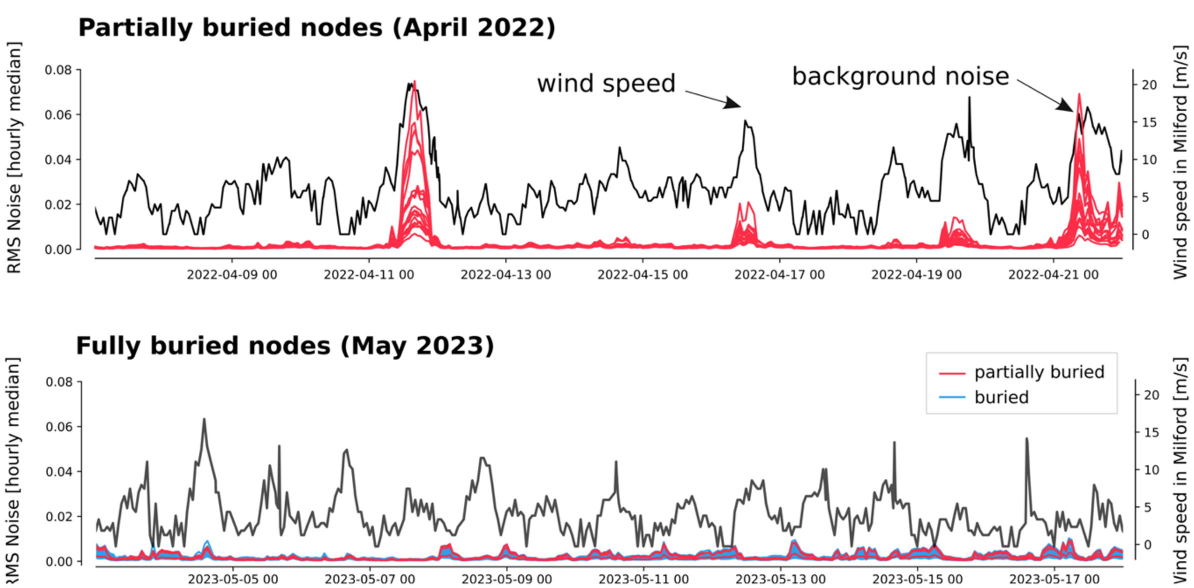

Figure 8. Wind speed (black line) and noise level recorded on nodal instruments (colored lines) for the 2022 (top) and 2023 (bottom) deployments. Red lines indicate partially buried instruments, and blue lines indicate completely buried instruments. In 2022, with all partially buried instruments, the instrument noise is high and correlates well with wind speed. In 2023, with mostly buried instruments, the noise level is lower and the correlation with wind is less pronounced.

6. CONCLUSIONS

Utah FORGE has demonstrated the strengths of multi-scaled seismic monitoring (Figure 9) and through experiment has innovated new strategies for seismic monitoring of EGS systems. Monitoring with seismic instrumentation in deep boreholes provides the highest precision seismic event catalogs. Considerations for reservoir-depth monitoring include: (1) acknowledging that the sensors and cables will be in an extreme environment and will likely fail in time. For longer term operations, Utah FORGE now limits the temperature to 150 °C for geophone deployment. Additionally, careful inspection of the complete systems before deployment is key for successful operation and having the capability to replace failed tools in the field is also important; (2) the ability to deploy DAS at reservoir temperature and its better spatial resolution provide key data for high precision seismic event location and for autolocation. However, DAS is less sensitive than geophones, so having at least one geophone together with DAS is important for monitoring lower magnitude events. It should also be borne in mind that the DAS response is not calibrated, so a geophone is always required for magnitude estimation; and (3) when integrating DAS because of the data volumes, one needs to carefully plan for data storage and processing, and parallelized codes are essential.

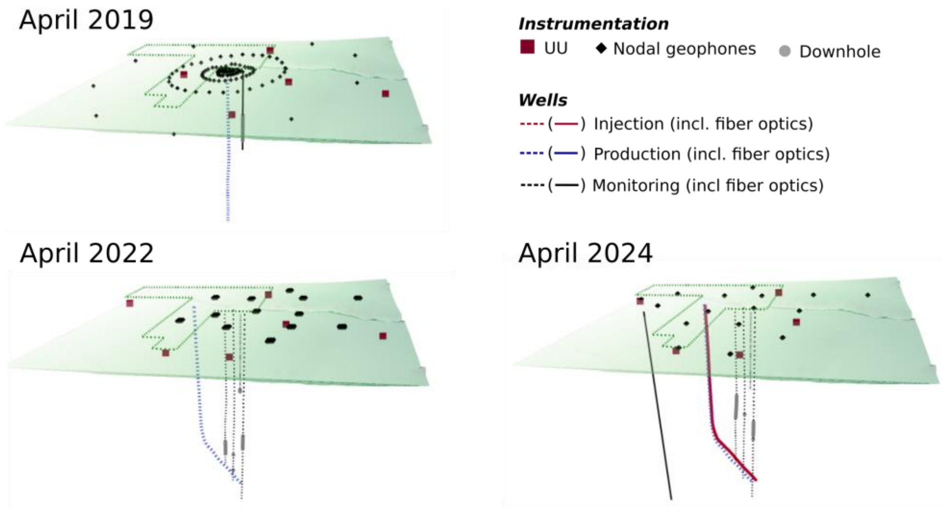

Figure 9: Summary figure showing the available seismic monitoring for the three Utah FORGE stimulations.

With enhanced processing and careful consideration of the noise sources, a near-surface network can provide a catalog of microseismicity within the reservoir. For example, the shallow 1000 ft borehole station FORK proved exceptionally valuable in detecting seismic activity during circulation and stimulation (Niemz et al., 2024; Niemz et al., 2025). The superior quality of the data recorded at station FORK compared to the other stations results from the effective noise reduction of the shallow borehole installation (Figure 10). Depending on resolution needs for event locations and duration of monitoring (e.g. only during operations or continuously) such installations may provide an optimized network with reduced drilling costs compared to deep borehole installations.

Lastly, large nodal geophone deployments provide a mechanism to address specific research questions and temporarily increase the focal sphere coverage. A downside of these deployments is there is no real-time monitoring. All processing is after instrument retrieval. When deploying such arrays, we demonstrate the advantage of deploying clusters of instruments in patches and the need to bury the instruments.

For commercial monitoring of EGS, there is now a benchmark to design seismic monitoring networks based on operational objectives. Before designing a seismic network, the objectives for seismic monitoring need to be identified. For TLS, a surface network is adequate, whereas for improved reservoir monitoring a network with surface and shallow boreholes combined with advanced processing could be utilized. For high resolution, seismic event detection and location reservoir depth geophones and/or DAS will produce the best results.

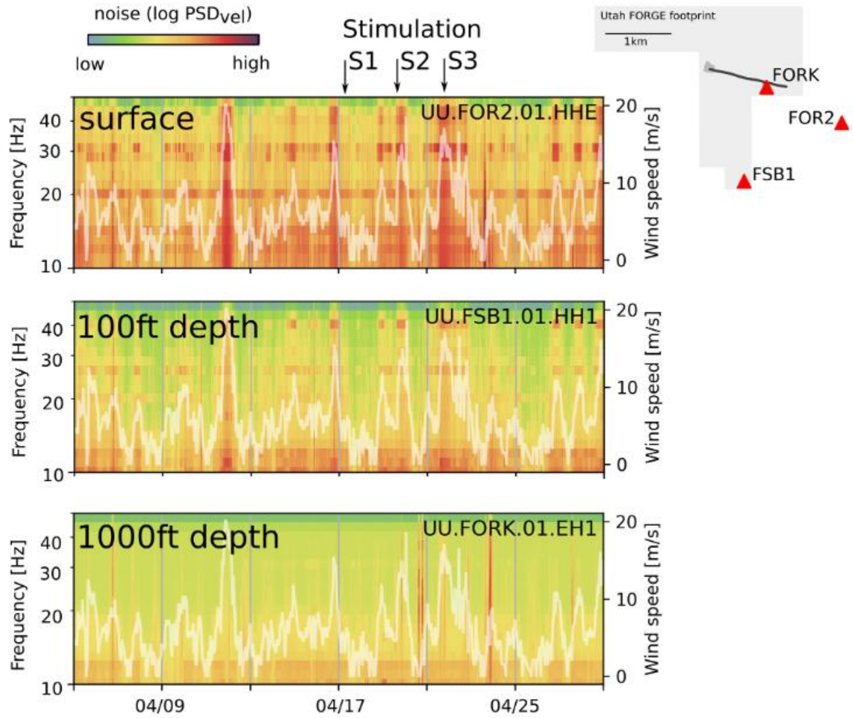

Figure 10: High winds (white line), common at Utah FORGE, can contaminate seismic records by introducing high background noise. Such noise contaminations affected the ability to detect low magnitude microseismic events, e.g., during the stimulation stages in April 2022 (Stages 1-3). The influence of surface noise induced by high winds is reduced significantly with the increasing installation depth of the sensors in a borehole. The wind and other noise sources vanish at a depth of 1000 ft, and local signals become more apparent.

7. ACKNOWLEDGEMENTS

We thank the University of Utah Field Engineers, Corey Hatch, Jon Rusho, Josh Alexander, Andy Trow, and Nick Forbes, for installing and maintaining the local seismic network. We thank Ryan Madsen and Aaron Becar for IT support on the Utah FORGE site. We also thank the many students and staff that have assisted in the nodal deployments. Funding for this work was provided by the U.S. DOE under grant DE-EE0007080 "Enhanced Geothermal System Concept Testing and Development at the Milford City, Utah FORGE Site." and by the Swiss Federal Office of Energy within the framework of the subsidy contract for the Haute Sorne project (contract MF_021-GEO-ERK). We thank the many stakeholders supporting this project, including the University of Utah, Smithfield, Utah School and Institutional Trust Lands Administration (SITLA), Beaver County, and the Utah Governor's Office of Energy Development.

REFERENCES

1. Bradshaw, P., G. Petersen, and K. Pankow: Utah FORGE: Orientation of Borehole and Surface Seismic Stations [data set] (2023). Retrieved from https://gdr.openei.org/submissions/1508.

2. Chet Hopp: *Cape Modern seismic monitoring network* [Data set] (2023). International Federation of Digital Seismograph Networks. https://doi.org/10.7914/m9sf-hx70.

3. Dyer, B.C., Schanz, U., Spillmann, T., Ladner, F., and Haring, M. O: Application of microseismic multiplet analysis to the Basel geothermal reservoir stimulation events. Geophysical Prospecting, 58, (2010), 791–807. doi: 10.1111/j.1365-2478.2010.00902.x.

4. Dyer, B., Karvounis, D., Bethmann, F.: Microseismic event catalogues from the well 16A(78)-32 stimulation in April, 2022 in Utah FORGE., ISC Seismological Dataset Repository, (2023a), https://doi.org/10.31905/52CC4QZB.

5. Dyer, B.C., Bethmann, F., Karvounis, D., Meier, P., Pankow, K., Wannamaker, P., Moore, J., Rutledge, J., and Ammon, A.: Innovative microseismic monitoring tools and configurations for geothermal applications, Proceedings World Geothermal Congress, Beijing, China, (2023b).

6. Finger, C., Niemz, P., Ermert, L., & Lanza, F.: Utah FORGE: Composite 3D Seismic Velocity Model. [Data set] (2024), https://dx.doi.org/10.15121/2305384, last accessed January, 2025

7. Freudenreich, Y., Oates, S. J., and Berlang, W.: Microseismic feasibility studies – assessing the probability of success of monitoring projects. Geophysical Prospecting, 60, (2012), 1043–1053.

8. Isken, M., P. Niemz, J. Münchmeyer, S. Heimann, S. Cesca, and T. Dahm (2025). Qseek: A data-driven Framework for Machine-Learning Earthquake Detection, Localization and Characterization, Seismica, Accepted for publication. Software available at: https://pyrocko.github.io/qseek/, last accessed January, 2025.

9. Lellouch, A., Lindsey, N.J., Ellsworth, W.L., and Biondi, B.L.: Comparison between Distributed Acoustic Sensing and Geophones: Downhole Microseismic Monitoring of the FORGE Geothermal Experiment. Seismological Research Letters, 91, (2020), 3256–3268. doi: https://doi.org/10.1785/0220200149.

10. Lellouch, A., Schultz, R., Lindsey,N.J., Biondi, B.L., and Ellsworth, W.L.: Low-magnitude seismicity with a downhole distributed acoustic sensing array – Examples from the FORGE geothermal experiment. Journal of Geophysical Research: SolidEarth, 126, (2021), e2020JB020462. https://doi.org/10.1029/2020JB020462.

11. Mesimeri, M., K. Pankow, and J. Rutledge: A frequency-domain-based algorithm for detecting microseismicity using dense surface seismic arrays, Bull. Seism. Soc. Am., 111, (2021a), 1-11, doi: 10.1785/0120210062.

12. Mesimeri, M., K. L. Pankow, W. D. Barnhart, K. M. Whidden, and J. M. Hale: Unusual seismic signals in the Sevier Desert, Utah possibly related to the Black Rock volcanic field, Geophys. Res. Lett., (2021b), https://doi.org/10.1029/2020GL090949.

13. Niemz, P., Petersen, G., Whidden, K. M., Pankow, K. L.: Exploring the potential of surface monitoring networks for induced seismicity in the Utah FORGE geothermal project, Oral Presentation at the XXVIII General Assembly of the International Union of Geodesy and Geophysics (IUGG), Berlin, Germany (2023). doi.org/10.57757/IUGG23-2796

14. Niemz, P., J McLennan, K. L. Pankow, J. Rutledge, and K. England: Circulation experiments at Utah FORGE: Near-surface seismic monitoring reveals fracture growth after shut-in, Geothermics, vol. 119, (2024), https://doi.org/10.1016/j.geothermics.2024.102947.

15. Niemz, P., K. L. Pankow, M. P. Isken, K. Whidden, J. McLennan, and J. Moore: Mapping fracture zones with nodal geophone patches: Insights from induced microseismicity during the 2024 stimulations at Utah FORGE, Seis. Res. Letts., (2025), https://doi.org/10.1785/0220240300.

16. Pankow, K. L., M. Stickney, J. Y. Ben-Horin, M. Litherland, S. Payne, K.D. Koper, S. L. Bilek, and K. Bogolub: Regional Seismic Monitoring in the Eastern Intermountain West, *Seism. Res. Lett.*, 91, (2019), 631-646, doi.1785/0220190209.

17. Pankow, K., J. Rutledge, and P. Niemz: Utah FORGE: Seismic Traffic Light System (Version 2), [dataset] (2025), Retrieved from https://gdr.openei.org/submissions/1706.

18. Pechmann, J. C., Nava, S. J., Terra, F. M., Bernier, J. C.; Local Magnitude Determinations for Intermountain Seismic Belt Earthquakes from Broadband Digital Data. *Bulletin of the Seismological Society of Americ*a, 97, (2007), 557–574. doi: https://doi.org/10.1785/0120060114

19. Petersen, G. M., S. Cesca, M. Kriegerowski, and the Alp Array Working Group: Automated quality control for large seismic networks: Implementation and application to the AlpArray Seismic Network, Seism. Res. Lett., 90, (2019),1177-1190.

20. Rutledge, J., Dyer, B., Wannamaker, P., Pankow, K., Bethmann, F., Meier, P., and Moore, J.: Downhole microseismic monitoring of injection stimulations at the Utah FORGE EGS site, 56th U.S. Rock Mechanics/Geomechanics Symposium, 2022.

21. Trow, A. J., K. L. Pankow, Y. Wang, F. C. Lin: Local ambient noise tomography over the FORGE Utah site, (eds.) R. Allis and J. Moore, Utah Geological Survey Misc. Pub. 169-G, (2019), doi:10.34191/MP-169.

22. Trow, A. J., H. Zhang, A. S. Record, K. A. Mendoza, K. L. Pankow, P. E. Wannamaker: Microseismic event detection using multiple geophone arrays in southwestern Utah, Seism. Res. Lett., 89, (2018), 1660-1670, doi:10.1785/0220180065.

23. Trugman, D. T. and P. M. Shearer: GrowClust: A Hierarchical Clustering Algorithm for Relative Earthquake Relocation, with Application to the Spanish Springs and Sheldon, Nevada, Earthquake Sequences. *Seismological Research Letters* 88, (2017), 379–391.

24. Trugman, D.T., Chamberlain, C. J., Savvaidis, A., Lomax, A.: GrowClust3D.jl: A Julia Package for the Relative Relocation of Earthquake Hypocenters Using 3D Velocity Models. Seismological Research Letters, 94 (1), (2022), 443–456.doi.org/10.1785/0220220193

25. Wells, D., F. C. Lin, K. Pankow, B. Baker, and J. Bartley: Combining dense seismic arrays and broadband data to image the subsurface velocity structure in geothermally active south-central Utah, J. Geophys. Res: Solid Earth, (2022), doi:10.1029/2022JB024070.

26. Whidden, K., G. Petersen, P. Bradshaw, A. Dzubay, and K. Pankow: Seismic monitoring of the 2022 Utah FORGE stimulation—the view from the surface, Stanford Geothermal Workshop, Pal Alto, California (2023).

27. Zhang, H. and K. L. Pankow: High-resolution Bayesian spatial auto-correlation (SPAC) pseudo-3D Vs model of Utah FORGE site with a dense geophone array, Geophys. Res. Int, (2021), https://doi.org/10.1093/gji/ggab049

APPENDIX 1: THE LOCAL SEISMIC NETWORK

The University of Utah Seismograph Stations (UUSS) has a modern regional earthquake catalog beginning in 1981 (Pankow et al., 2019). UUSS has also operated stations in and near to the Milford Valley since the mid-1980's. During early stages (2019 – 2020) of the Utah FORGE project a temporary network of broadband stations was installed (Figure A1.1) to better characterize local seismicity. Beginning in late-2020, UUSS began to transition from temporary monitoring to a dedicated local seismic network. This build out was completed in 2022 (Figure A1). The network consists of surface and shallow borehole instrumented locations with a mix of broadband, geophone and accelerometer sensors. Table A1 describes the metadata. An issue when installing instruments in shallow boreholes is determining the orientation for the horizontal sensors. At Utah FORGE, we processed surface waves from teleseismic earthquakes using AutoStatsQ (Petersen et al., 2019). This analysis is described in Bradshaw et al. (2023) and the orientation for horizontal channel 1 is given in Table A2.

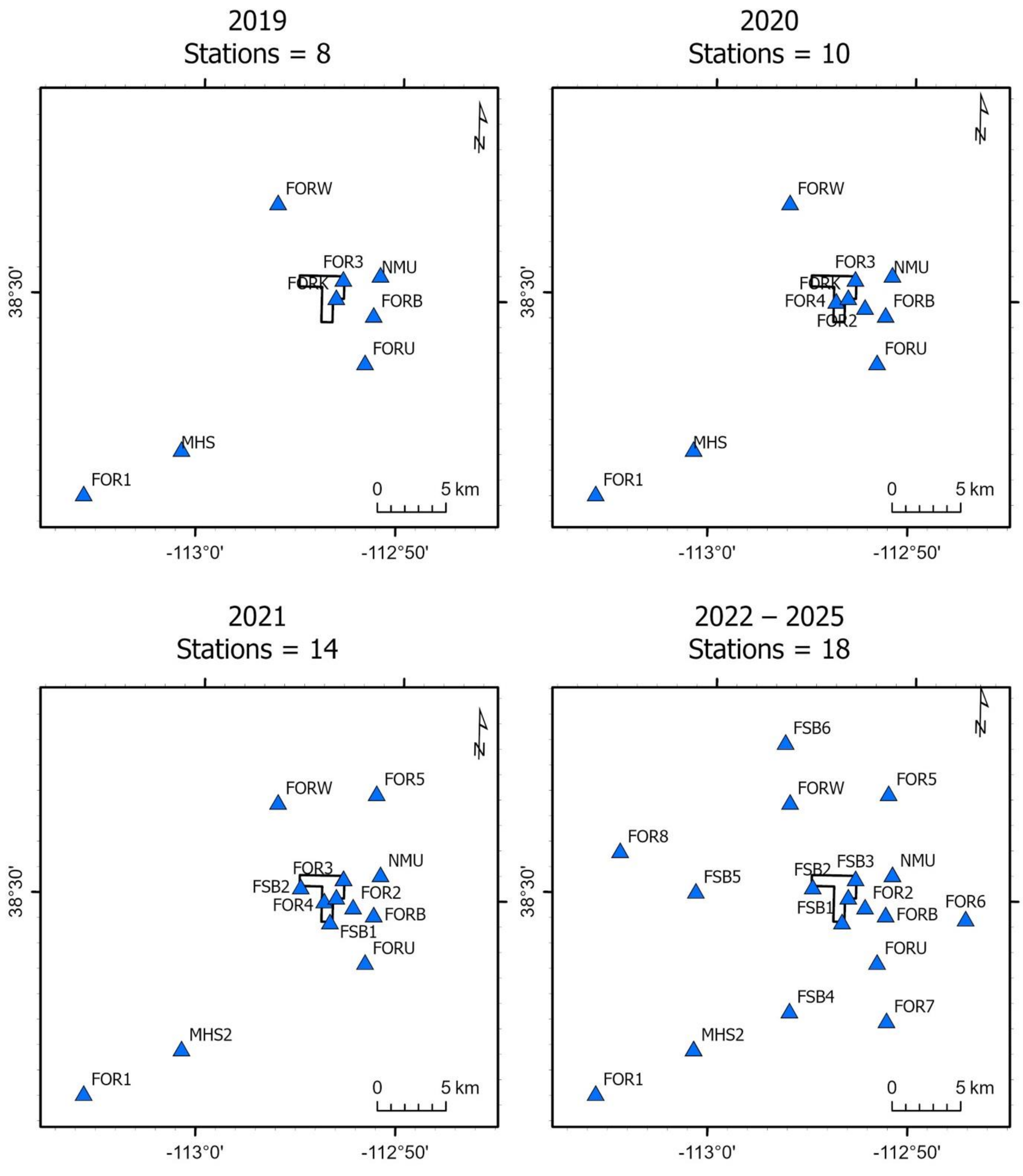

Figure A1.1: Evolution of the local seismic network at Utah FORGE. Blue triangles, stations.

Table A1.1: Seismic station metadata

Type	SEED Name	Depth	Datalogger	Sensor	Sample Rate
Shallow borehole	UU.FORK.EH[Z,1,2] UU.FORK.GH[Z,1,2] UU.FORK.EN[Z,1,2] UU.FORK.GN[Z,1,2]	~305 m (~1000')	Obsidian	OMNI-2400 (short-period) Silicon Audio (accelerometer	200 sps 1000 sps 200 sps 1000 sps
Shallow borehole	UU.FSB[1,2,3].HH[Z,1,2] UU.FSB[1,2,3].EN[Z,1,2] UU.FSB[1,2,3].DN[Z,1,2]	~30 m (~100')	Centaur	Trillium Cascadia (broadband) Titan (accelerometer)	200 sps 200 sps 500 sps
Shallow borehole	UU.FSB[4,5,6].HH[Z,1,2]	~40 m (~140')	Centaur	Trillium Compact PH (broadband)	200 sps
Rock Site	UU.FOR[1,5,6,7,8].HH[Z,E,N]	Surface	Centaur	Trillium 120, 120[Q,P]A, or Horizon (broadband)	200 sps
Soil Site	UU.FOR2.HH[Z,E,N]	Surface	Centaur	Trillium 120 (broadband)	200 sps
Rock Site	UU.FORU.HH[Z,E,N]	Surface	Centaur	Trillium Compact PH (broadband)	200 sps
Strong-motion	UU.[FORB,FORW] .EN[Z,E,N]	In-building	Basalt Obsidian	Episensor	200 sps
Strong-motion	UU.MHS2.EN[Z,E,N]	In-building	Etna2	Episensor	100 sps

Table A1.2: Shallow borehole horizontal component orientation

Station	Channel 1 Azimuth degrees from North
FORU	-1
FSB1	-104
FSB2	118
FSB3	23
FSB4	-142
FSB5	42
FSB6	40

APPENDIX 2: THE BOREHOLE SEISMIC NETWORK

Here we summarize the deep borehole instrumentation configurations deployed as part of operations for the purpose of detecting and accurately locating low-magnitude (Mw < -1.0) events induced during various reservoir development operations implemented from 2019 though 2024. We present the planned deployments, guided by modeling and project objectives and summarize the executed deployments and data acquired.

A2.1 2019 April – Pilot stimulation in well 58-32

Operational goal: Can we create fractures? Can we detect stimulation-induced microseismicity near and above the granite / basin-fill interface?

A pilot injection test was conducted in April and May 2019 in well 58-32. A test monitor well, 78-32, was placed close to the pilot injector, 58-32 and drilled to 3280 ft into the top of granite (2615 ft). Schlumberger deployed their 12-level VSI digital receiver string spanning the top of granite from 2115 to 3215 ft. The initial objective of the seismic monitoring was to measure microseismic sensitivity of small events near the top of granite and up through the overlying, basin-fill sediments. Injection depths in 58-32 were at 6560 to 7545 ft, approximately 4400 ft beneath the geophone string. Schlumberger detected and located up to 424 small events with moment magnitudes, Mw, ranging from -2 to 0. The Schlumberger 3C waveform data are of good quality. However, the single-well monitoring geometry, with the receivers placed high above the microseismic source area, results in very poor location accuracy.

Silixa deployed a DAS cabled behind the 78-32 casing from TD to surface. A careful study was conducted directly comparing the side-by-side responses of the geophone and DAS strings (Lellouch et al., 2020; Lellouch et al., 2021).

A2.2 2022 April—May – Initial injection stimulations of 16A(78)-32

Operational Goals - map the stimulated volumes

Well 16A(78)-32 was initially stimulated with three injection stages placed near the toe section. Downhole microseismic monitoring involved the use of the 58-32 well plus the drilling of two additional deep wells (56-32 and 78B-32) dedicated primarily for the monitoring of these initial injection stimulations of 16A(78)-32. The locations of wells 56-32 and 78B-32, relative to 58-32, were based on Utah FORGE leasing options and on modeling of the detection sensitivity and event location accuracy, with emphasis on targeting the toe section of 16A(78)-32 and the consideration of the geophone strings deployed in the three wells (Rutledge et al., 2022).

Due to instrumentation problems, stages 1 and 2 were only monitored with a single, 3C, 8-level string set in well 58-32, spanning depths of 5880 to 6580 ft. Monitoring the stage-2 treatment did include the addition of a two-level string placed in 56-32 with sensor depths at 7272 and 8272 ft. However, the time-release locking arms on the geophone sondes were not deployed, thus degrading the signal fidelity and noise levels. The best receiver coverage was obtained for the stage-3 stimulation with the deployment of three vertical, multi-level downhole geophone strings providing a total of eighteen 3C geophone receivers deployed within or just above the target reservoir (Figure A2.1). Wells 58-32 and 78B-32 each had 700 ft long, 8-level, 3C strings placed approximately 1500 and 2000 ft above the 16A(78)-32 injection depths. A two-level analog string was placed in well 56-32 with the lowest geophone set at reservoir depth and the upper receiver anchored 1000 ft above (Figure A2.1). The downhole microseismic catalog for the April 2022 injection stimulations can be obtained at the ISC Seismological Dataset Repository (Dyer et al., 2023a).

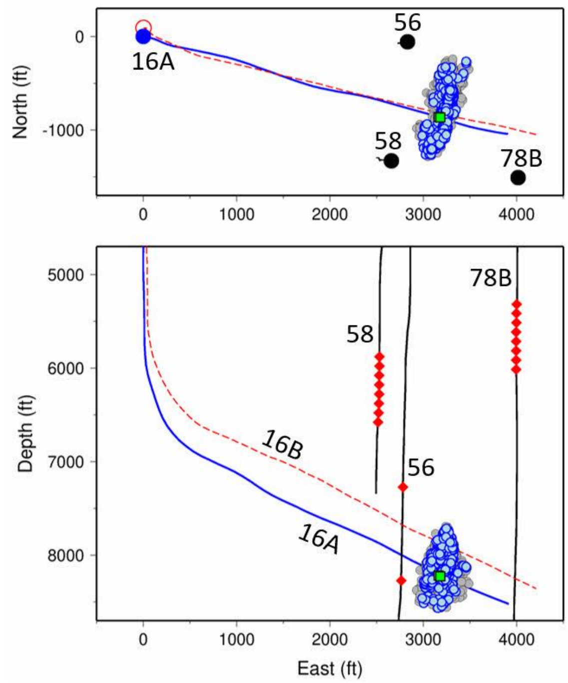

Figure A2.1: Microseismic event locations for the stage 3 stimulation completed in well 16A(78)32 (top, map view; bottom, cross-section). The entire population of located events are shown in gray, consisting of 5283 events with moment magnitudes(Mw) ranging from -2.0 to 0.6 (Dyer et al., 2023a; Dyer et al., 2023b). The events shown in blue are a subset (1120 events) with higher magnitudes Mw ≥ *-0.85. The 3-component geophone receivers are shown as red diamonds in monitor wells 58-32, 78B-32, and 56-32. The location of the 16A(78)32 stage-3 stimulation perforation interval, which was 20 ft long, is shown with the green square. The 16B(78)-32 well, shown as a red dashed line, was drilled after the stage-3 stimulation.*

A2.3 2023 July Circulation test

Operational Goals - are the injection and production wells connected

In July 2023, water was injected into 16A(78)-32,through stages 1, 2, and 3 that were stimulated in April 2022. A small quantity of fluid was produced from 16B(78)-32. Data was collected with a DAS system for the bottom 3845 ft of the behind-casing Prysmian fiber in 16B(78)-32 (803 channels). After the circulation, the data was deconvolved with a Gauge Length of 1.5 meter, resampled from 4kHz to 2kHz and eventually processed by GeoEnergie Suisse (GES). A total of 2223 events were detected during the period 15-20 of July 2023. For 884 of these events, the minimum distance from 16B(78)-32 and the MD of the nearest 16B(78)-32 could be estimated. Data from other monitoring wells was not processed.

A2.4 2024 April – 16A(78)-32 and 16B(78)-32 Stimulation

Operational Goals - develop an EGS reservoir

Monitoring during April 2024, covered the stimulations of 16A(78)-32 and 16B(78)-32. During this period, the downhole microseismic network consisted of: 1) a single-level 3C analog geophone in 56-32; 2) an 8-level, 700-ft length, 3C, digital string made by Avalon in 78B-32; 3) a behind-casing DAS system in 16B(78)-32 (1496 channels); and 4) a behind-casing DAS system in monitoring well "Delano" on Fervo's Cape Modern project area south of the 16A/B(78)-32 pad (1317 channels). Schlumberger also deployed a 12-level (1100 ft length) 3C digital string in well 58-32. However, Schlumberger was unable to convert and transmit their data stream in a useful format in real time to the GES seismic trailer; hence, their data was never integrated into the larger downhole seismic network. After stage 7 was pumped in well 16A(78)-32, water started to flow to the surface in well 58-32 and Schlumberger pulled out of the hole and ceased their monitoring operations. Before the flow to surface occurred in well 58-32, Schlumberger had multiple tool failures from the high temperatures. Consequently, they were only able to record a discontinuous, and incomplete catalog of events on a string that was not always oriented due to missing calibration (perforation) shots.

After the stimulations in wells 16A(78)-32 and 16B(78)-32 were completed, GES deployed a wireline DAS in well 58-32 and successfully integrated the DAS channels into their larger downhole receiver network during post-injection monitoring.

A2.7 2024 August – Month long circulation test

An extended circulation test was conducted at the Utah FORGE site between August 8 and September 5, 2024. During this one-month period, the single level PSS in 56-32 and the DAS system monitoring the Delano well (622 traces) recorded seismic data with minimal interruptions. The two-level PSS was deployed on the 14th of August. DAS utilized for monitoring was behind casing fiber in 16B(78)-32. The single mode fiber 2 in the FIMT (SMF2) fiber was monitored until the 16th of August for MD 5081 ft-9791 ft, and then for the range MD 370.3 ft-5080.6 ft, always with 706 traces. The depth change was necessary because the bottom part of the fiber had degraded. On the 21st of August, the monitoring of SMF2 finished and the IU was connected to the Carina fiber on the Silixa cable behind casing in 16B(78)-32 (MD 4151-6786 ft, 760 traces). All DAS systems acquired data at 1 kHz, and the PSS at 2 kHz.

APPENDIX 3: NODAL GEOPHONE EXPERIMENTS REFERENCES

Here we summarize (Table 3.1) the nodal experiments conducted by Utah FORGE. More details on the experiments can be found in the references for each experiment. The data is available through the EarthScope DMC.

Table A3.1: Nodal geophone experiments.

Date	Geometry	References
2016 December	44 nodes in ~4 km grid 49 nodes in ~650 m grid	Trow et al., 2018 Trow et al., 2019 Zhang et al., 2021 Wells et al., 2022
2017 August	49 nodes in ~650 m grid (reoccupied)	Trow et al., 2018
2019 April	5 km aperture circular array 151 nodes on rings with radii ranging from 100 to 2500 m	Mesimeri et al. 2021a Mesimeri et al., 2021b
2022 April	208 nodes in 13 patches of 16 nodes. Patches 4 x 4 grid, 30 m spacing	Whidden et al., 2023
2023 May	76 nodes in 2 patches of 38 nodes. Patch grids had spacings of 5-, 10-, and 20 m	*This paper*
2024 April	144 nodes in 16 patches of 9 nodes. Patches 3 x 3, 10 m spacing	Niemz et al., 2025